PROCEEDINGS OF SCIENCE

The charge response study of LHAASO-WCDA large spherical PMTs

Bo Gao,[a,*] **Congcong Liu,**[a] **Lin Liu,**[a] **Mingjun Chen,**[a] **Kai Li**[a] **and Xiaohao You**[a]

[a] *Institute of High Energy Physics,*
19 B Yuquan Road, Shijingshan Di strict, Beijing, China

E-mail: gaobo@ihep.ac.cn

The charge response of the detector is very important for data reconstruction and energy spectrum analysis. In this paper, the charge response of LHAASO large size PMT is studied in depth, including the difference in detection efficiency between MCP and Dynode structure PMTs, and a calibration charge nonlinear method based on continuous optical attenuator is proposed. After the correction from charge calibration, the experimental data can reach a good agreement with the simulation results.

38th International Cosmic Ray Conference (ICRC2023)
26 July - 3 August, 2023
Nagoya, Japan

*Speaker

PoS(ICRC2023)801

1. Introduction

Large size photomultiplier tubes (PMT) are widely used in astro-particle physics and neutrino physics experiments due to their large effective detection area and good time resolution[1]. In the LHAASO experiment, 2220 20-inch MCP-PMT with "Lotus-like" focusing electrode structure (see in Fig. 1) are applied in the water Cherenkov detector array (WCDA)[2]. It is used to detect the Cherenkov photons generated by the secondary particles of cosmic ray shower in water, converting Cherenkov light pulses to electric pulses. By measuring the timing and intensity of the light flashes produced by the water, WCDA can determine the energy and direction of the cosmic rays that pass through it. This information can be used to study the properties of cosmic rays and the high-energy processes that produce them[4].

However, the response of MCP-PMT varies greatly under different magnetic fields, so the magnetic effect is necessary to be studied[3]. Because of the large size, PMT can not be simply treated as a point[5], and the research on the response under different positions of PMT is very helpful for us understanding the detector.

Since 2 types of large PMTs are applied in LHAASO-WCDA, one is 20-inch MCP-PMT and the other is well studied 8-inch dynode PMT manufactured by Hamamatsu, in order to conduct data analysis and normalization in the later stage, the charge response of the two types of PMT must also be studied.

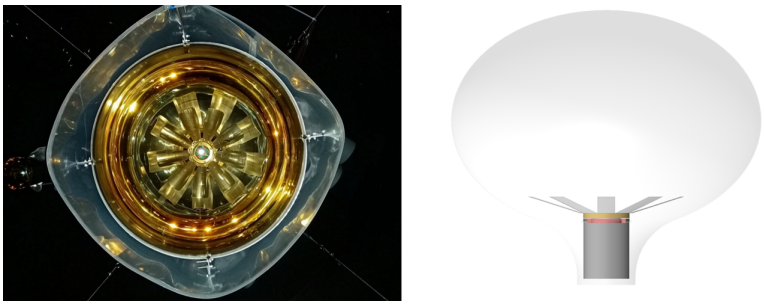

Figure 1: The 20 inch MCP PMT. Left : top view; Right : structure side view.

2. The scanning system

A scanning system is built for the test mentioned above, it is composed of three parts: 1) mechanical motion device; 2) Light source; 3) Control and data acquisition system. The diagram is shown in Fig. 2. The scanning sequence is shown in Fig. 3.

3. Data analysis and system resolution

The MCP PMT responses under different magnetic field are evaluated by detection efficiency, output charge, relative transit time (RTT) and transit time spread (TTS).

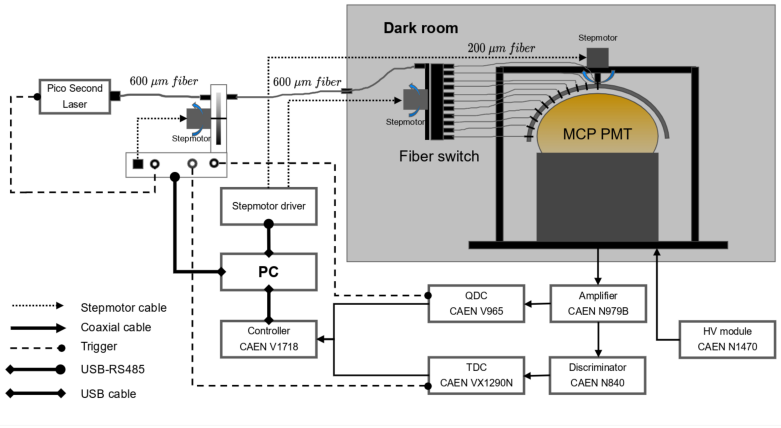

Figure 2: The scanning diagram.

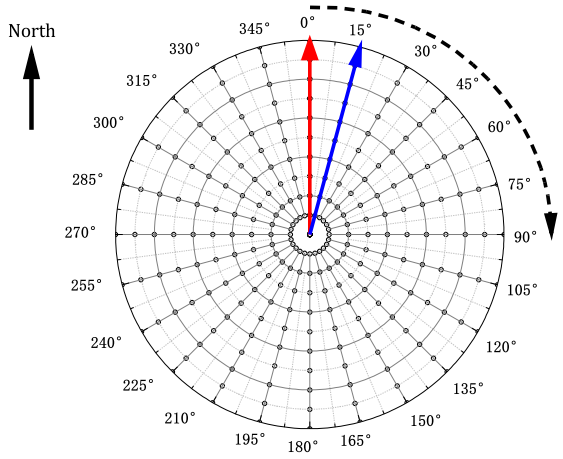

Figure 3: Scanning sequence with top view of the MCP PMT.

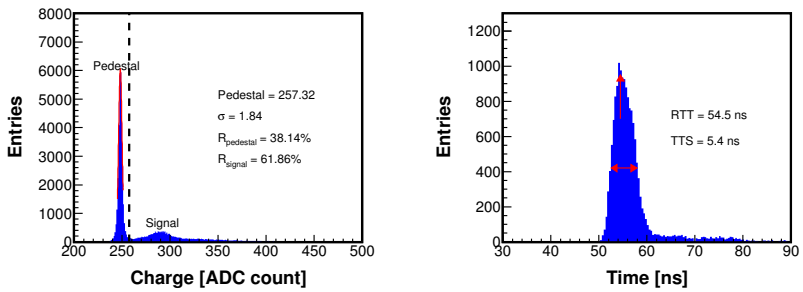

Figure 4: Charge and arrival time distribution at low light intensity.

3.1 Data analysis

Take the center point at low light intensity and magnetic shielding condition test as example, Fig. 10 shows the charge spectrum and arrival time result. In the charge spectrum, the left part of the dotted line is pedestal region, the mean value of pedestal and width (σ) of the pedestal is obtained by Gaussian fitting, the dotted line position corresponds to $pedestal + 5.0\sigma$, the detection efficiency (DE) is defined as the data ratio in signal region, in this distribution, the DE is 38.14%. With the increase of light intensity, it is obvious that the detection efficiency will rise to the maximum of 100%.

The relative transit time is defined as the most probable value of the time distribution, and TTS is evaluated as the FWHM of the distribution. When the signal probability is 100%, PMT charge can be defined as the average of charge distribution minus the pedestal. When the trigger probability is less than 100%, the probability of number of photon electrons follows Poisson distribution, that is, the effective charge is the weighted average of non-zero signal. Take charge distribution in Fig.10 as example, at low light intensity, the effective charge is calculated as follows:

$$Q_{mean} = Q \times DE \tag{1}$$

The scanning system resolution is mainly composed of the stability of PMT, light source and the coupling uncertainty of optical fiber switch[6]. In the scanning procedure, the fixed point $\{\theta, \phi\} = \{0°, 0°\}$ are tested 25 times, and the test time interval is also uniform, so the data of this point can be used to evaluate the system accuracy. Fig. 5 shows the accuracy of each parameters under low light intensity. It can be seen that the accuracy of the overall system is as follows: the

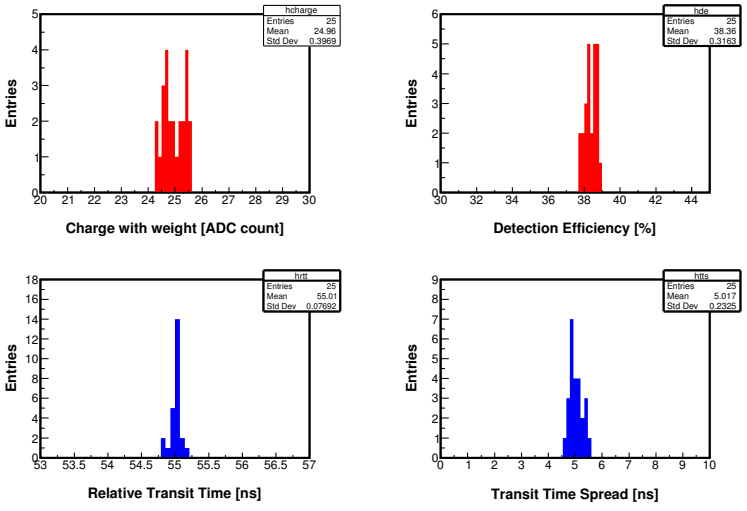

Figure 5: System accuracy at low intensity with magnetic shield.

precision of the charge test is within 0.39% , the precision of detection efficiency is within 0.32% , the stability of relative transit time and transit time spread is within 76.9 ps and 0.23 ns. At the same time, compared with the data at a certain light intensity in the Result section, the minimum charge uniformity is around ±40%, the distribution of detection efficiency values is at a minimum of around 10% , the distribution of RTT and TTS are at a minimum of around 40 ns and 5 ns.

This indicates that the scanning system's accuracy is good enough to meet the test precision, which makes the data can appropriately reflect the MCP-PMT's characteristics.

4. Test result

4.1 Charge reponse by scanning

To study the response of various parameters such as RDE, anode uniformity, RTT, TTS, under different light intensities, 11 sets of light intensity values were used in the test by using the continuous neutral density filter, and the output photon number of a single fiber ranged from a few photons to thousands of photons.

In order to describe the differences in various positions more vividly, we selected a set of data under low light intensity and 9 positions on the PMT for illustration. As it is shown in Fig.6, point O is the center of the PMT, and point A to H located at an elevation angle of 45° and an azimuth angle ranging from 0° to 315° with a step size of 45°.

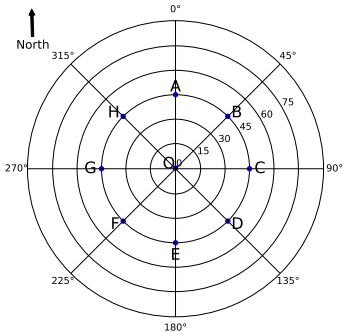

Figure 6: Selected points on PMT surface.

4.1.1 Relative detection efficiency

Relative detection efficiency is one of the important parameters that characterize the detection capability of a PMT.It is calculated as the ratio of the number of detected photons by the PMT to the number of incident photons generated by the light source.

As described above, Fig.7 shows the charge spectrum distribution of 9 positions under the same low light intensity. It can be clearly seen the detection efficiency and charge distribution spectrum vary significantly under without shielding condition(Blue). However, the variation in charge spectrum and detection efficiency are relatively small under magnetic shielding condition(Red).

Similarly, the 2-D distribution and 1-D statistical information of the detection efficiency for all scanning points are shown in Fig.8 under without/with magnetic shielding conditions.

4.1.2 Anode charge non-uniformity

The plot of charge distribution is presented in the top line of Fig. 9. It can be seen that the geomagnetic effect has a significant impact on PMT, causing significant differences in different positions. After adding magnetic shielding, the overall trend tends to be more consistent. To

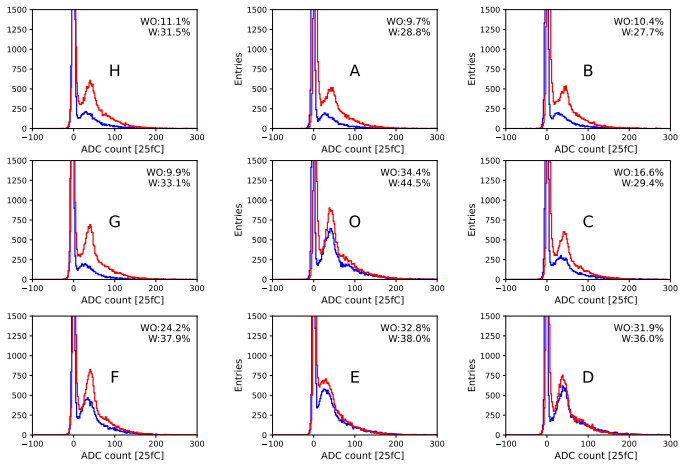

Figure 7: Charge spectrum of selected points.

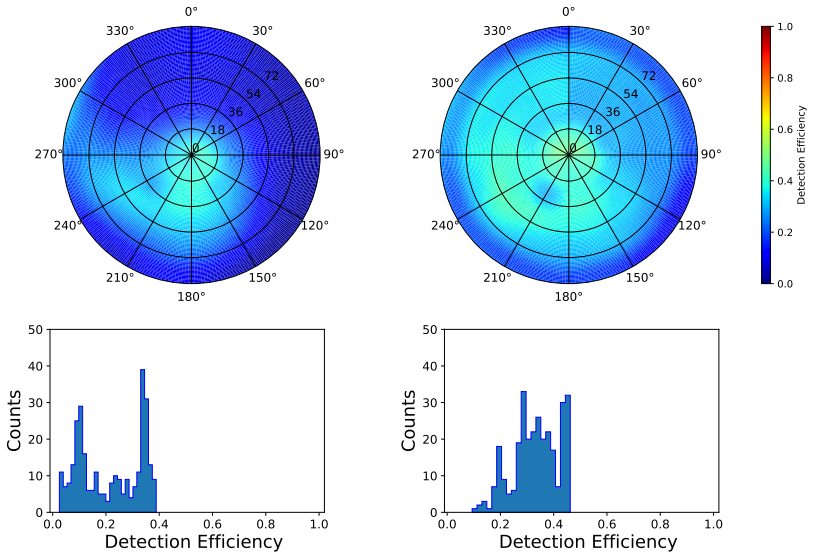

Figure 8: (Top,left):DE without shielding. (Top,right):DE with shielding. (Bottom,left):Numerical distribution of DE without shielding.(Bottom,ight):Numerical distribution of DE with shielding.

achieve uniformity, the charge value of each position was divided by the average value of the overall charge,which can be expressed as follows:

$$\Delta = \frac{Q \times DE}{Q_{mean}} - 1 \tag{2}$$

The bottom row displays the one-dimensional numerical distribution of the non-uniformity in MCP PMT at the same intensity. It can be seen that the charge uniformity distribution width of the PMT changes from ±100% to ±50% after the addition of the magnetic shield, the uniformity of charge distribution is greatly improved. /subsectionCharge reponse comparison to dynode PMT Due to the use of two different multiplication structures in the PMTs, the charge response of the two PMTs needs to be normalized during the data analysis process. In the test, we focused on studying the

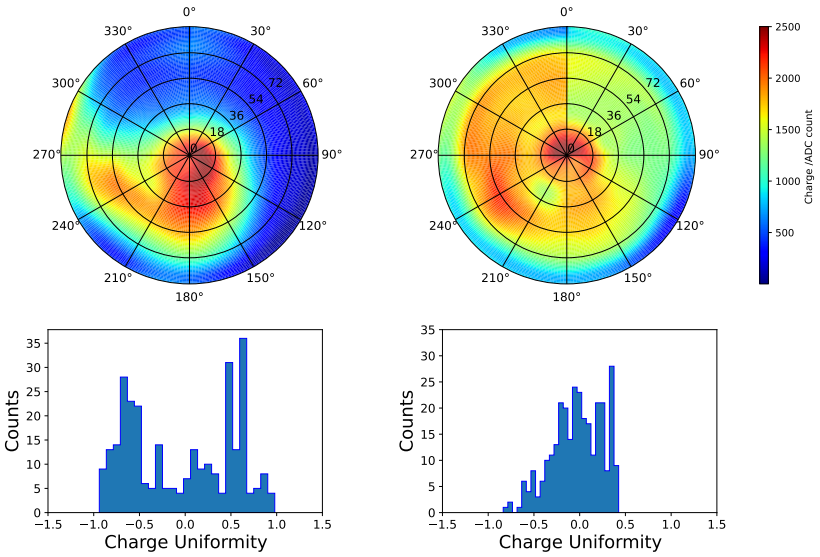

Figure 9: (Top,left): Charge distribution without shielding. (Top,right): Charge distribution with shielding. (Bottom,left): Numerical distribution of charge uniformity without shielding. (Bottom,right): Numerical distribution of charge uniformity with shielding.

behavior of the charge response under low light intensity. First we measured the charge spectra of 8-inch dynode PMT and 20-inch MCP-PMT with different gains under the same light intensity conditions (Fig. reffig:spe), one should notice that the pedestal and main peak in the distribution are set to 0 and 1 seprately. The experimental results show that there is a significant difference in the charge response of the two PMTs at low light intensities. This is because of the multiplication structure of the MCP. When a photocathode generates a photoelectron and it is accelerated and falls onto the MCP, there is a certain probability that it directly enters the microchannel and undergoes multiplication, 65% in this type of MCP PMT. Alternatively, it may hit the surface of the microchannel plate, resulting in the first multiplication. The number of secondary electrons produced after the first multiplication depends on the voltage, and the probability of these secondary electrons falling into adjacent microchannels depends on their generation position and direction. It is evident that the second scenario introduces significant uncertainty in the signal output at the anode of the MCP-PMT. This leads to nonlinearity in multiplication at low light intensities. As the light intensity increases, when the triggering probability reaches 100%, the output exhibits a fixed multiplication factor. Through measurements, the additional multiplication factor is approximately 30%.

5. Conclusion

3120 large spherical PMTs are applied in LHAASO-WCDA, including 900 8-inch dynode PMTs and 2220 20-inch MCP PMTs. The charge reponse under geo-magnetic field and comparison between 2 types of PMTs are tested, the results provides support for better data analysis and make more deeply understanding.

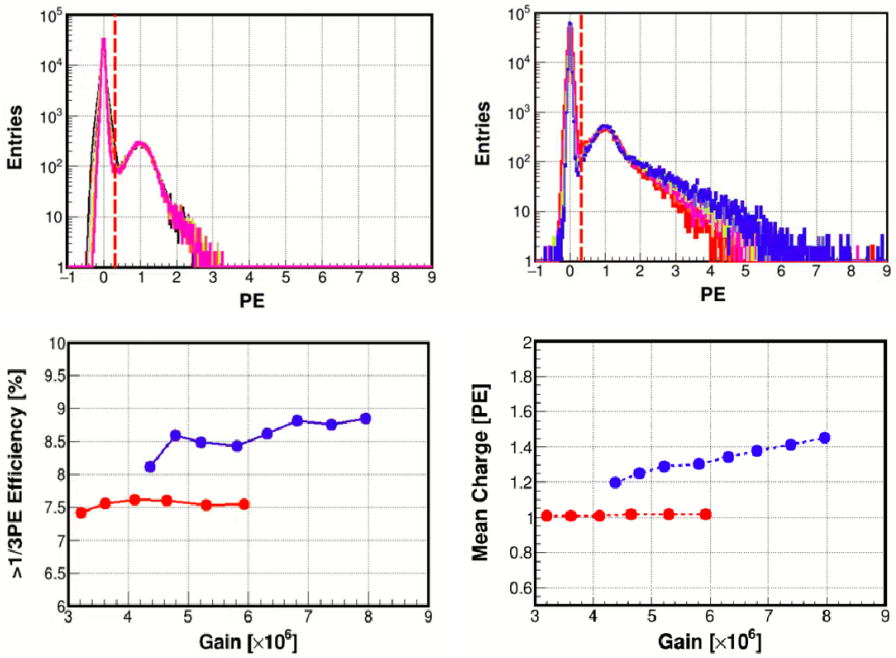

Figure 10: (Top,left): 8-inch dynode PMT SPE charge spectrum under different gains. (Top,right): 20-inch dynode PMT SPE charge spectrum under different gains. (Bottom,left): Relative detection efficiency under fixed low light intensity. (Bottom,right): Weighted charge under different gains.

References

[1] Cao Zhen et al., *Introduction to Large High Altitude Air Shower214 Observatory (LHAASO)* , *Chin. Astron. Astrophys.* **43** (4) (2019) 457-478.

[2] Huihai He et al., *Design of the LHAASO detectors Radiat. Detect. Technol. Methods* **2** (2018) 1-8.

[3] O. Smirnov et al., *Magnetic shielding for large photoelectron multipliers for the OSIRIS facility of the JUNO detector* , *JINST* **18** (04) (2023) P04015.

[4] Angel Abusleme et al., *Mass testing and characterization of 20-inch PMTs for JUNO Eur. Phys. J. C* **82** (2022).

[5] Feng Gao et al., *Research and development of 20-inch PMT uniformity scanning platform* , *Nucl. Instrum. Meth. A* **1027** (2022) 166257.

[6] Ling Ren et al., *Study on the improvement of the 20-inch microchannel plate photomultiplier tubes for neutrino detector* , *Nucl. Instrum. Methods Phys. Res. A* **977** (2020) 0168-9002.

[7] You X H et al., *The Application of 20 inch MCP-PMT in LHAASO-WCDA Proc.37th Int. Cosmic Ray Conf* (2021).

[8] W. P. Huang et al., *An accurate measurement of PMT TTS based on the photoelectron spectrum* , *Chinese Physics C* **39** (2015) 066003.